

# PI3K/AKT pathway alterations are associated with clinically aggressive and histologically anaplastic subsets of pilocytic astrocytoma

Erika F. Rodriguez · Bernd W. Scheithauer · Caterina Giannini ·  
Amanda Rynearson · Ling Cen · Bridget Hoesley · Heather Gilmer-Flynn ·  
Jann N. Sarkaria · Sarah Jenkins · Jin Long · Fausto J. Rodriguez

Received: 23 September 2010/Revised: 24 October 2010/Accepted: 16 November 2010/Published online: 28 November 2010  
© Springer-Verlag 2010

**Abstract** Pilocytic astrocytomas (PA) are well-differentiated gliomas having a favorable prognosis when compared with other diffuse or infiltrative astrocytomas. Molecular genetic abnormalities and activation of signaling pathways associated with clinically aggressive PA and histologically anaplastic PA have not been adequately studied. We performed molecular genetic, gene expression, and immunohistochemical studies using three PA subsets, including conventional PA ( $n = 43$ ), clinically aggressive/recurrent PA ( $n = 24$ ), and histologically anaplastic PA ( $n = 25$ ). A clinical diagnosis of NF1 was present in 28% of anaplastic PA. Molecular cytogenetic studies demonstrated

heterozygous *PTEN*/10q and homozygous *p16* deletions in 6/19 (32%) and 3/15 (20%) cases of anaplastic PA, respectively, but in neither of the two other groups. *BRAF* duplication was identified in 33% of sporadic anaplastic PA and 63% of cerebellar examples. *BRAF*<sup>V600E</sup> mutation was absent in four (of 4) sporadic cases lacking duplication. *IDH1*<sup>R132H</sup> immunohistochemistry was negative in 16 (of 16) cases. Neither *PDGFRA* nor *EGFR* amplifications were present. pERK staining levels were similar among the three PA subsets, but a stepwise increase in cytoplasmic pAKT and to a lesser extent pS6 immunoreactivity was noted by immunohistochemistry in aggressive PA groups. This was particularly true in histologically anaplastic PA when compared with conventional PA ( $p < 0.001$  and  $p = 0.005$ , respectively). In addition, *PTEN* expression at the mRNA level was decreased in histologically anaplastic PA when compared to the other groups ( $p = 0.05$ ). In summary, activation of the PI3K/AKT in addition to MAPK/ERK signaling pathways may underlie biological aggressiveness in PA. Specifically, it may mediate the increased proliferative activity observed in histologically anaplastic PA.

**Electronic supplementary material** The online version of this article (doi:10.1007/s00401-010-0784-9) contains supplementary material, which is available to authorized users.

E. F. Rodriguez · B. W. Scheithauer · C. Giannini ·  
A. Rynearson · J. Long · F. J. Rodriguez  
Department of Anatomic Pathology and Laboratory Medicine,  
Mayo Clinic, 200 First Street, SE, Rochester, MN 55905, USA

L. Cen · J. N. Sarkaria  
Department of Radiation Oncology, Mayo Clinic,  
Rochester, MN, USA

B. Hoesley · H. Gilmer-Flynn  
Advanced Genomics Technology Center, Mayo Clinic,  
Rochester, MN, USA

S. Jenkins  
Biomedical Statistics and Informatics, Mayo Clinic,  
Rochester, MN, USA

F. J. Rodriguez (✉)  
Division of Neuropathology, Department of Pathology,  
Johns Hopkins University, 720 Rutland Avenue,  
Ross Building 512B, Baltimore, MN 21205, USA  
e-mail: faustorodriguez232@hotmail.com; frodrig4@jhmi.edu

**Keywords** Pilocytic astrocytoma · Brain ·  
Neurofibromatosis · Glioma · PTEN · AKT

## Introduction

Pilocytic astrocytoma (PA) is a well-differentiated astrocytoma occurring most frequently in children and young adults. Compared to diffuse or infiltrative astrocytomas, PA is associated with a favorable prognosis, 5-year survival rates being >95% after gross total resection [19]. Histologically, it is characterized by the presence of a biphasic

pattern including compact, fibrillary tissue featuring Rosenthal fibers and loosely arranged, microcyst-rich tissue containing eosinophilic granular bodies.

Despite its favorable prognosis, approximately 20% of PA patients experience tumor recurrence or clinical progression [5]. A subset may result in significant morbidity or mortality, despite lack of atypical histologic features. Conversely, histologically anaplastic PAs are less frequent. These were defined in our previous study as PA demonstrating hypercellularity, moderate to severe cytologic atypia, and brisk mitotic activity with or without necrosis [25]. So defined, anaplasia was associated with decreased survival, corresponding to those of infiltrative astrocytomas of grades II and III, depending if necrosis was absent or present, respectively.

In recent years, our molecular understanding of gliomas has greatly increased. Activation of the MAPK/ERK and PI3K/AKT pathways are hallmarks of a variety of malignancies, including high-grade astrocytomas [18]. Genetic alterations frequently involved, include amplification of genes encoding for receptor tyrosine kinases (*EGFR*, *PDGFRA*) and deletions/mutations in tumor suppressor genes (*TP53*, *p16*, *PTEN*) [18].

Recently, genetic alterations involved in the development of low grade astrocytomas such as PA have also been uncovered by high resolution genomic studies. MAPK/ERK pathway activation through aberrations of *BRAF* and *RAF1* in sporadic PA or the *NF1* gene in neurofibromatosis type 1 (NF1)-associated PA are most frequent [1, 6, 8, 13, 15, 22, 31]. Our present study evaluates the status of MAPK/ERK and PI3K/AKT pathways in PA subsets and explores their association with clinical and histological aggressiveness.

## Materials and methods

### Patients and tissue microarrays

Primary tumors were studied using primarily two tissue microarrays, including conventional PA ( $n = 43$ ), clinically aggressive/recurrent PA ( $n = 24$ ), and histologically anaplastic PA ( $n = 25$ ). Median patient age and gender were 13 years (M 20; F 23), 23 years (M 14; F 10), and 29 years (M 17; F 8) for the three groups, respectively. Clinical criteria for NF1 were present in 11 (26%), 1 (4%), and 7 (28%) cases, respectively. Anatomical sites for conventional, aggressive and histologically anaplastic PA, respectively, included optic pathway/hypothalamus (21, 13, 0%), supratentorial CNS (37, 42, 36%) and infratentorial CNS (42, 46, 64%).

Aggressive/recurrent PA was defined as PA progressing within a year of surgery despite adequate therapy or requiring additional surgical intervention, but lacking histologic features of anaplasia. Histologically anaplastic PAs were obtained predominantly from the consultation files from one of us (BWS); their clinicopathologic features were the subject of our previous publication [25]. Their morphologic characteristics were summarized above. The tissue microarrays were constructed using 0.6 mm diameter cores per tumor in triplicate. All studies were approved by the Institutional Review Board and Biospecimen committee at Mayo Clinic.

### Fluorescence in situ hybridization

All fluorescence in situ hybridization (FISH) studies were performed upon formalin-fixed, paraffin-embedded tissue microarray or whole tissue sections using previously described methods [26]. Locus-specific probes targeted the following regions: *EGFR* (7p12, Abbott Molecular/Vysis), *P16* (9p21, Abbott Molecular/Vysis), *PTEN* (10q23, Abbott Molecular/Vysis), *PDGFRA* (Custom Made) and *BRAF* (Custom Made with clones RP4-592P3, RP4-726N20, RP5-839B19, RP4-813F11) (7q34). All target probes were labeled with SpectrumOrange™ (Abbott Molecular/Vysis, Des Plaines, Ill). Respective reference probes (CEP 4, 7, 9, 10) were labeled with SpectrumGreen™. A minimum of 100 non-overlapping nuclei were assessed per case. Chromosomal losses and gains were evaluated using previously established cutoffs [26]. The identity of the BACs used to construct the custom-made *BRAF* probe was confirmed with PCR analysis (Supplementary Fig. 1).

### *BRAF*<sup>V600E</sup> mutation analysis

Five cases with sufficient material for DNA extraction were used for *BRAF*<sup>V600E</sup> mutation analysis. Four to six 10- $\mu$ m paraffin sections were used for genomic DNA extraction by the phenol:chloroform:isopropyl alcohol (Invitrogen) method. A 224-bp fragment of *BRAF* gene exon 15 was amplified using the following PCR primers: 5'-TCATAA TGCTTGCTCTGATAGGA (forward) and 5'-GGCCAAA AAT TTAATCAGTGGA (reverse), as previously reported [17]. PCR products were separated on a 2% agarose gel and visualized by ethidium bromide staining. Aliquoted products were used for bidirectional DNA sequencing on an ABI Prism 377 DNA Sequencer (PE Applied Biosystems, Foster City, CA, USA). NPA (thyroid tumor) cell lines with a known *BRAF*<sup>V600E</sup> mutation and PTC1 cells with a known wild type *BRAF* genotype were used for controls.

## Real-time RT-PCR

Total RNA was extracted from 5 to 10 sections of formalin-fixed paraffin-embedded tissue, each 10  $\mu\text{m}$  thick, using the RecoverALL™ Total Nucleic Acid Isolation Kit (Applied Biosystems). Quantitation of gene expression was performed using Taqman gene expression assays (Applied Biosystems), including *PTEN* (Hs02621230\_s1) and *BRAF* kinase domain (Hs01052468\_g1), *GAPDH* serving as an endogenous control. A total of 100–1,000 ng of total RNA were converted to cDNA, 10 ng loaded per well. Tumor and control brain samples were run in triplicate on the ABI 7900HT Fast real-time PCR system (Applied Biosystems) using 96-well plates. Data analysis was performed using  $\Delta\Delta\text{Ct}$  method with SDS software according to the manufacturer's recommendations (<http://www.appliedbiosystems.com>).

## Immunohistochemistry

Immunohistochemical studies were performed using a Dako autostainer and the Dual Link Envision+ or ADVANCE detection systems on 5- $\mu\text{m}$  thick formalin-fixed, paraffin-embedded tissue microarray sections. Antibodies applied were directed against AKT (total) (Rabbit polyclonal, 1:500 dilution, cell signaling technology), pAKT (clone736E11 recognizing phospho-ser473 site, 1:800; cell signaling technology), pERK (Rabbit polyclonal Erk1/2) (Thr202/Tyr204; 1:250 cell signaling technology); pS6 (Rabbit polyclonal p-S6 (Ser235/236) 1:200, cell signaling technology); EGFR (2-18C9, prediluted; Dako), p53 protein (clone DO7, 1:2,000; Dako), IDH1<sup>R132H</sup> (Clone H09, 1:50, Dianova), and ki67 (clone MIB-1, monoclonal, 1:300; Dako). Cytoplasmic staining for EGFR, AKT, pAKT, and pERK were scored on a four-tier semi-quantitative scale by two observers as previously described [26]. Nuclear stains (p53, ki67) were quantitatively estimated using the Hamamatsu NanoZoomer Digital Pathology scanning and IHCscore software for computer-assisted analyses.

## Statistical analysis

Survival rates were described using Kaplan–Meier curves and analyzed with Cox proportional hazard regression. The time to event was defined as time from surgery to death (or last follow-up if censored). Fisher's exact tests were used to compare proportions, and the Student's *t*, Wilcoxon rank sum, or Kruskal–Wallis tests were used to compare continuous variables between groups of interest. Statistical analyses were performed using SAS version 9 or JMP version 8 software (SAS Institute, Inc., Cary, NC). *P* values <0.05 were considered statistically significant.

## Results

### Molecular genetic abnormalities of histologically anaplastic PA

The molecular genetic abnormalities observed in this subset of tumors are summarized in Table 1 and are illustrated in Fig. 1.

### *PTEN* and *p16*

Molecular cytogenetic analysis demonstrated heterozygous *PTEN* (10q) deletions in 6/19 (32%) histologically anaplastic PA but in none of 39 conventional or clinically aggressive PA ( $p < 0.001$ ). Whole chromosome 10 loss was not observed. Homozygous deletions of *p16* were noted in 3/15 (20%) histologically anaplastic PA but in none of 16 conventional or clinically aggressive PA. These alterations were present both in the histologically anaplastic component and PA precursor when tested (2 cases with *PTEN* deletion and one with *p16* deletion). All *p16* homozygous deleted tumors had *PTEN* deletions. However, three *PTEN*-deleted tumors had intact *p16* loci (Table 2).

### *BRAF*

Duplication of *BRAF* was present in 5/15 (33%) sporadic histologically anaplastic PA (mean *BRAF*/*CEP7* ratio 1.38), but in none of two NF1 associated histologically anaplastic PA tested. The frequency of *BRAF* duplication was highest in cerebellar examples (5/8) (63%) cases, and limited to this anatomic location. Conversely, proportional gains/polysomies of chromosome 7 were more frequent (15/21 cases (71%)). In addition, *BRAF* duplication was present in (16/40) (40%) sporadic PA without anaplasia. Re-examination of histologically anaplastic PA lacking *BRAF* duplication demonstrated convincing classical histological features of conventional PA in these tumors (Fig. 2), arguing against the alternative diagnosis of infiltrating glioma.

Because of the increased frequency of polysomies in histologically anaplastic PA when compared with the other groups, we performed qRT-PCR analysis using primers targeting RNA coding for the *BRAF* kinase domain to see if increasing copy number was associated with gene overexpression. There were no differences in *BRAF* expression levels noted among the groups ( $p > 0.05$ ).

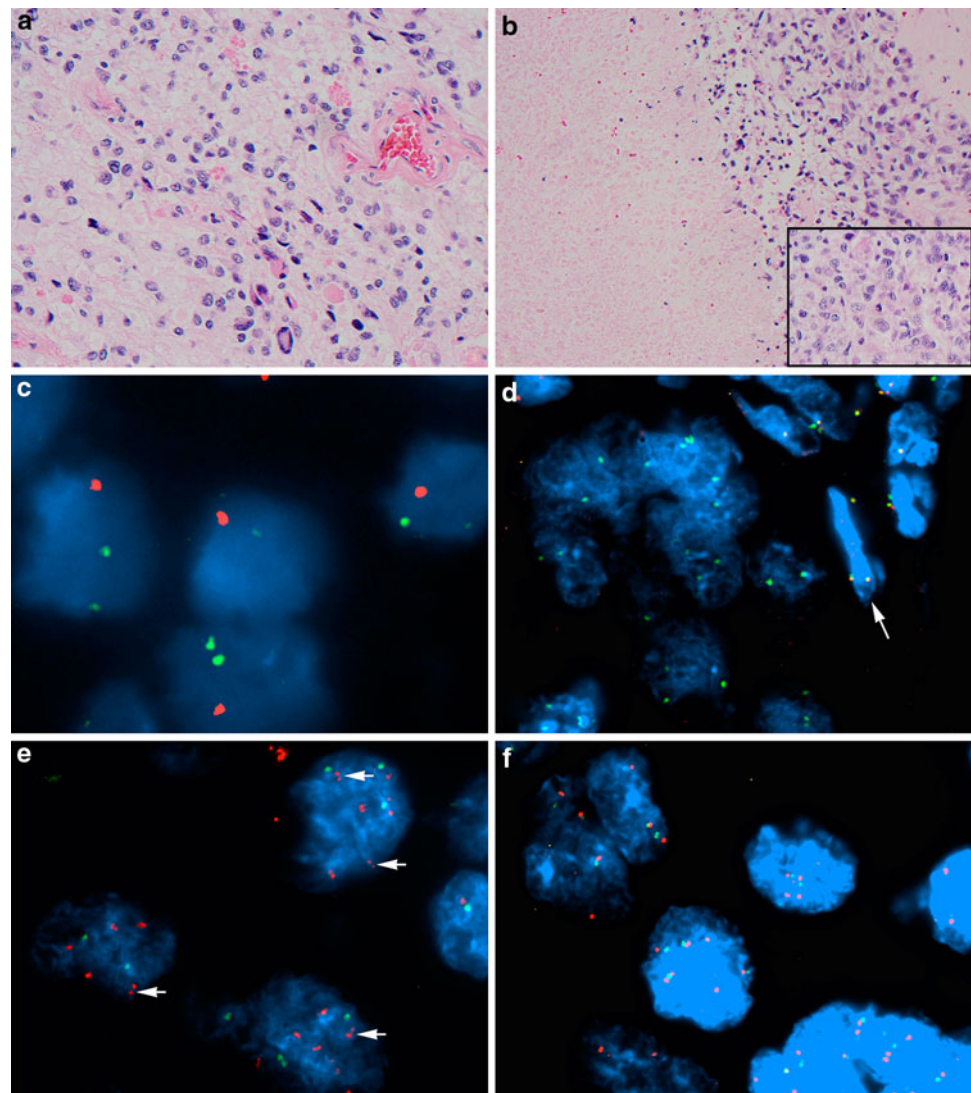
Testing for *BRAF*<sup>V600E</sup> mutation by DNA sequencing was successfully performed in four sporadic histologically anaplastic PA lacking *BRAF* duplication. This demonstrated wild type *BRAF* (Supplementary Fig. 2).

**Table 1** Molecular genetic features in 22 cases of histologically anaplastic PA

Case	Age	Sex	Location	NF1 clinical status	History of radiation	Necrosis	PTEN	BRAF	BRAF V600E	Chr7	P16	PDGFRA	EGFR	IDH <sup>R132H</sup> IHC
1	5	M	Cerebellum	Sporadic	No	No	NA	Dup	NA	Normal	Normal	No Amp	No Amp	Neg
2	70	M	Cerebellum	Sporadic	No	Yes	Het del	Normal	NA	Normal	HD	No Amp	No Amp	Neg
3	28	M	Cerebellum	Sporadic	Yes	Yes	WT	NA	NA	+7	NA	NA	No Amp	Neg
4	11	M	R frontal lobe	Sporadic	No	Yes	WT	Normal	WT	+7	Normal	No Amp	No Amp	Neg
5	36	F	Cerebellum	Sporadic	No	No	Het del	Dup	NA	+7	Normal	No Amp	No Amp	Neg
6	29	M	Cerebellum	NF1	No	No	Het del	Normal	NA	Normal	HD	No Amp	No Amp	Neg
7	20	M	Cerebellum	Sporadic	No	Yes	WT	Dup	NA	+7	Normal	No Amp	NA	Neg
8	27	M	Cerebellum	Sporadic	Yes	Yes	Het del	Dup	NA	+7	HD	No Amp	NA	Neg
9	75	M	L temporal lobe	Sporadic	No	No	WT	Normal	WT	+7	Normal	No Amp	No Amp	Neg
10	10	M	3rd ventricle	Sporadic	No	Yes	WT	Normal	NA	+7	Normal	No Amp	No Amp	Neg
11	39	F	Cerebellum	Sporadic	Yes	Yes	NA	Dup	NA	+7	Normal	No Amp	No Amp	Neg
12	46	M	L parietal lobe	NF1	No	Yes	WT	NA	NA	Normal	NA	NA	No Amp	Neg
13	46	F	R temporal lobe	NF1	No	No	WT	Normal	NA	+7	Normal	No Amp	NA	Neg
14	73	F	Tectum	Sporadic	No	Yes	WT	Normal	WT	+7	Normal	No Amp	No Amp	Neg
15	51	M	Spinal cord	Sporadic	No	No	Het del	Normal	NA	Normal	Normal	NA	No Amp	Neg
16	19	M	Cerebellum	NF1	No	No	WT	NA	NA	Normal	NA	NA	No Amp	NA
17	26	M	Cerebellum	NF1	No	Yes	WT	NA	NA	+7	NA	NA	No Amp	NA
18	16	M	Spinal cord	Sporadic	No	Yes	Het del	Normal	NA	+7	Normal	No Amp	No Amp	NA
19	49	F	Cerebellum	Sporadic	No	Yes	WT	Normal	NA	+7	NA	No Amp	No Amp	NA
20	21	F	Medulla	Sporadic	No	Yes	WT	Normal	WT	+7	Normal	No Amp	No Amp	NA
21	33	M	L parietal lobe	NF1	No	No	WT	NA	NA	+7	NA	NA	No Amp	NA
22	55	F	Cerebellum	Sporadic	NA	No	NA	Normal	NA	+7	NA	NA	NA	NA

NF1 neurofibromatosis type 1, *Het del* heterozygous deletions, *HD* homozygous deletions, *WT* wild type, *Chr* chromosome, *No Amp* no amplification, *Neg* negative, *NA* test failed or not done

**Fig. 1** Molecular genetic alterations in histologically anaplastic PA. Case 8: Conventional PA component characterized by astrocytes with degenerative atypia, hyalinized vasculature and numerous eosinophilic granular bodies (a). Features of anaplasia in PA include coagulative necrosis (b) and brisk mitotic activity (inset). Molecular alterations included heterozygous *PTEN* deletions (c), homozygous *p16* deletions (arrow points to a non-neoplastic endothelial cell with preservation of both *p16* loci) (d), and *BRAF* duplications (arrows) in association with polysomies (e). Amplifications of receptor tyrosine kinases were not identified, although proportional chromosomal gains/polysomies were frequent (f)



#### *PDGFRA* and *EGFR*

*PDGFRA* or *EGFR*, two cell surface receptor tyrosine kinases, are often amplified in pediatric and adult high-grade astrocytomas, respectively. Neither was present in the histologically anaplastic PA tested (0/15 and 0/18, respectively). Nonetheless, increased EGFR protein immunoreactivity was noted in aggressive PA and histologically anaplastic PA as compared to conventional PA ( $p = 0.05$  and  $0.02$ , respectively).

#### *IDH1*<sup>R132H</sup>

To exclude the possibility of histologically anaplastic PA representing progression from a diffuse glioma, immunohistochemistry using an antibody recognizing the most frequent mutant protein, *IDH1*<sup>R132H</sup>, was performed and was negative in 16 (of 16) cases tested.

Activation of the *PI3K/AKT* signaling pathway is associated with an aggressive PA phenotype

#### *PTEN* gene expression

Given the increased frequency of *PTEN* heterozygous deletions present in histologically anaplastic PA, we hypothesized that the *PI3K/AKT* pathway may be differentially activated in this subset of tumors as compared to conventional PA. Upon evaluating tumors for *PTEN* gene expression, *PTEN* mRNA levels were decreased in histologically anaplastic PA relative to PA without anaplasia ( $p = 0.05$ ) (Wilcoxon Rank Sum) (Fig. 3). As a group, *PTEN* mRNA levels were approximately twofold lower in histologically anaplastic when compared with non-anaplastic PA. With the caveat that subgroups within the histologically anaplastic PA group were small, we found no differences in *PTEN* gene expression levels between

**Table 2** Alterations of the MAPK/ERK and PI3K/AKT pathways in histologically anaplastic PA ( $n = 25$ ), clinically aggressive PA ( $n = 24$ ), and conventional PA ( $n = 43$ )

Case #	Age	Sex	Location	NF1 clinical status	Tumor type	<i>PTEN</i> FISH	<i>PTEN</i> qRT-PCR FC FINAL	pAKT IHC	pS6 IHC	<i>BRAF</i> FISH	pERK IHC	<i>P16</i> FISH
1	5	M	Cerebellum	Sporadic	APA		1.07	2	2	Dup	3	Normal
2	70	M	Cerebellum	Sporadic	APA	Het Del		2	2	Normal		HD
3	28	M	Cerebellum	Sporadic	APA	WT		2	3		2	
4	11	M	R frontal lobe	Sporadic	APA	WT	-13	3	3	+7	3	Normal
5	36	F	Cerebellum	Sporadic	APA	Het Del	-19	1	3	Dup + 7	3	Normal
6	29	M	Cerebellum	NF1	APA	Het Del	-3.9	2	3	Normal	3	HD
7	20	M	Cerebellum	Sporadic	APA	WT		1	2	Dup	2	Normal
8	27	M	Cerebellum	Sporadic	APA	Het Del	1.9	2	3	Dup	2	HD
9	75	M	L temporal lobe	Sporadic	APA	WT		2	1	+7	3	Normal
10	10	M	3rd ventricle	Sporadic	APA	WT		3	2	+7	3	Normal
11	39	F	Cerebellum	Sporadic	APA		-1.44	3		Dup		Normal
12	46	M	L parietal lobe	NF1	APA	WT	-6	2			0	
13	46	F	R temporal lobe	NF1	APA	WT	-3.6	0	0	+7	3	Normal
14	73	F	Tectum	Sporadic	APA	WT	-7	2		+7	3	Normal
15	51	M	Spinal cord	Sporadic	APA	Het Del	-1.75	2	3	Normal		Normal
16	19	M	Cerebellum	NF1	APA	WT						
17	26	M	Cerebellum	NF1	APA	WT						
18	16	M	Spinal cord	Sporadic	APA	Het Del		2		+7		Normal
19	49	F	Cerebellum	Sporadic	APA	WT				0		
20	21	F	Medulla	Sporadic	APA	WT		2		+7		Normal
21	33	M	L parietal lobe	NF1	APA	WT						
22	55	F	Cerebellum	Sporadic	APA			3		+7		
23	41	M	Pineal region	Sporadic	APA		-1.9					
24	11	F	R occipital lobe	NF1	APA				3		3	
25	14	M	Posterior fossa	Sporadic	APA				0	Failed		
26	39	F	Cerebellum	Sporadic	Agg PA	WT		1	0	Normal	3	
27	4	F	Suprasellar	Sporadic	Agg PA			2	0	Dup	3	
28	28	M	3rd ventricle	Sporadic	Agg PA			0		Normal	2	
29	32	M	R lat ventricle	Sporadic	Agg PA	WT		1	3	+7	3	
30	10	M	R parietooccipital	Sporadic	Agg PA	WT		0	0	Dup		
31	23	F	4th ventricle	Sporadic	Agg PA	WT		1	1	+7	3	
32	4	F	R thalamus	NF1	Agg PA							
33	6	F	L frontal lobe	Sporadic	Agg PA	WT		0	2	Normal	3	Normal
34	26	M	R temporoparietal	Sporadic	Agg PA	WT		2	0	+7	3	Normal
35	50	M	Cerebellum	Sporadic	Agg PA							
36	39	F	L frontal lobe	Sporadic	Agg PA			0	0		3	Normal
37	1	F	Posterior fossa	Sporadic	Agg PA	WT	-1.56	2	2	Dup	3	Normal
38	42	F	L temporal lobe	Sporadic	Agg PA	WT	-1.05	2	0	Dup	3	Normal
39	44	M	R frontal lobe	Sporadic	Agg PA	WT		2		Dup	3	Normal
40	6	F	Posterior fossa	Sporadic	Agg PA	WT		2	3	Normal	2	Normal
41	18	M	Cerebellum	Sporadic	Agg PA	WT		1	0	Dup	2	Normal
42	37	M	Cerebellum	Sporadic	Agg PA			2		Normal	3	Normal
43	23	F	L thalamus	Sporadic	Agg PA	WT	1.04	2	1	Normal	3	Normal
44	22	M	3rd ventricle	Sporadic	Agg PA	WT	-2.3	2	3	Dup	2	Normal
45	7	M	3rd ventricle	Sporadic	Agg PA	WT		1	3	Normal	2	Normal
46	3	M	Cerebellum	Sporadic	Agg PA			0	0			Normal
47	34	M	Posterior fossa	Sporadic	Agg PA				3			
48	2	M	Cerebellum	Sporadic	Agg PA				2			Normal
49	23	M	R temporal lobe	Sporadic	Agg PA		-2.6			Normal		

**Table 2** continued

Case #	Age	Sex	Location	NF1 clinical status	Tumor type	<i>PTEN</i> FISH	<i>PTEN</i> qRT-PCR FC FINAL	pAKT IHC	pS6 IHC	<i>BRAF</i> FISH	pERK IHC	<i>P16</i> FISH
50	7	F	L temporal lobe	Sporadic	PA			1	0	Normal	2	
51	17	M	L frontal lobe	NF1	PA	WT	-1.72	2	2	Normal	3	
52	14	F	3rd ventricle	Sporadic	PA	WT		2	2	Normal	2	
53	13	M	R frontal lobe	NF1	PA	WT	1.64	2	2	Normal	3	
54	33	M	Spinal cord	Sporadic	PA	WT			0	Failed	2	
55	10	M	Cerebellum	NF1	PA		-2.56	0	3	Normal	3	
56	22	M	R parietal lobe	Sporadic	PA	WT		0	0	Normal	2	
57	9	F	Suprasellar	Sporadic	PA			1	0	Normal	2	
58	14	F	R temporal lobe	Sporadic	PA	WT		0	0	Normal		
59	18	F	Cerebellum	Sporadic	PA	WT		0	0	Normal	2	
60	2	M	L optic nerve	NF1	PA		-1.78					
61	21	M	L parietooccipital	Sporadic	PA	WT		1	0	Dup	2	
62	5	M	Posterior fossa	Sporadic	PA	WT		1	0	Normal	2	
63	21	F	Temporal lobe	NF1	PA			1	3	Normal	3	
64	5	F	L optic nerve	NF1	PA			0			2	
65	2	F	L lat ventricle	NF1	PA			0	0	Normal	2	
66	30	F	R lat ventricle	NF1	PA			0	3	Normal	3	
67	18	F	Cervicomedullary	Sporadic	PA	WT		0	2	Dup	2	
68	4	M	Posterior fossa	Sporadic	PA	WT		0	0	Normal	2	
69	16	M	Posterior fossa	Sporadic	PA	WT		2	3	Normal	3	
70	58	M	L frontotemporal	Sporadic	PA		-2.6			+7		
71	11	F	Midbrain	Sporadic	PA				0	Dup	2	
72	1	F	Posterior fossa	Sporadic	PA	WT		0	0	Dup	2	
73	37	M	L frontal lobe	Sporadic	PA	WT			2	+7	3	
74	37	F	L thalamus	Sporadic	PA				2		3	
75	13	F	Posterior fossa	Sporadic	PA	WT		1	3	Normal	3	
76	5	F	Suprasellar	Sporadic	PA	WT		0	1	Dup	2	
77	12	M	R thalamus	Sporadic	PA			0	1	Normal	3	
78	46	F	Cerebellum	Sporadic	PA	WT		1	0	Dup	2	
79	18	F	3rd ventricle	Sporadic	PA				3	Normal	3	
80	47	F	Hypothalamus	Sporadic	PA			1	0	+7	3	
81	4	M	Cerebellum	Sporadic	PA	WT		1	0	Dup	3	
82	19	M	4th ventricle	Sporadic	PA	WT		0	0	Dup	1	
83	7	M	Suprasellar	Sporadic	PA	WT		0	1	Normal	3	
84	11	F	Posterior fossa	Sporadic	PA	WT		1	0	Dup	3	
85	3	F	R optic nerve	NF1	PA			0	0		1	
86	2	M	Suprasellar	Sporadic	PA			2		Dup	3	
87	3	F	Cerebellum	Sporadic	PA	WT		0	0	Dup	2	Normal
88	13	M	R temporooccipital	NF1	PA	WT		1	3	+7	3	Normal
89	45	F	Brainstem	NF1	PA			0	0		2	
90	3	M	Cerebellum	Sporadic	PA		-1.7			Normal		
91	19	M	4th ventricle	Sporadic	PA		3.66			Dup		
92	76	F	Cerebellum	Sporadic	PA		-2.6			Normal		
93	40	M	L temporal lobe	Sporadic	Control	WT	1	0	0	Normal	0	
94	52	M	L temporal lobe	Sporadic	Control	WT	6.428604	0	0	Normal	0	
95	1	F	Cerebellum	Sporadic	Control	WT		0	1	Normal	0	

*NF1* neurofibromatosis type 1, *Het del* heterozygous deletions, *HD* homozygous deletions, *WT* wild type

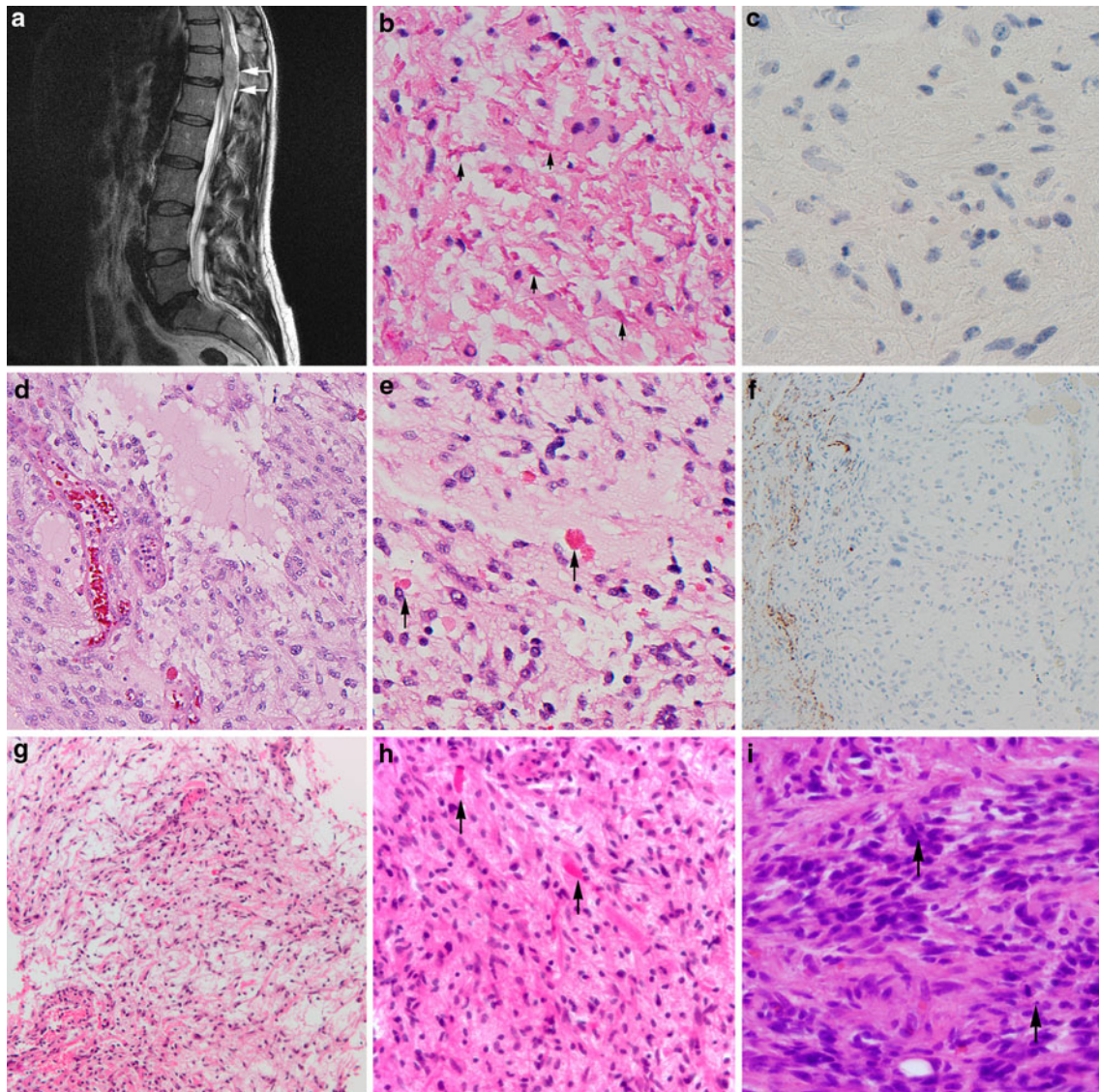


**Fig. 2** Histologically anaplastic PA lacking *BRAF* duplication have morphological components identical to conventional PA. Case 15: Well circumscribed spinal cord neoplasm in a 51-year-old man (**a**); histological review demonstrates numerous Rosenthal fibers (*arrows*) in a relatively circumscribed astrocytoma with piloid cells (**b**); immunohistochemistry for *IDH1*<sup>R132H</sup> was negative (**c**). Case 4: Histologically anaplastic PA involving the frontal lobe of an 11-year-old male with prominent microcysts and hyalinized vessels (**d**);

eosinophilic granular bodies were also present (*arrows*) (**e**); neurofilament protein immunostain highlights compressed axons at the periphery of the tumor consistent with a solid architecture (**f**); Case 6: Loose textured tumor with microcysts involving the cerebellum of a 29-year-old with NF1 (**g**); Rosenthal fibers were present in other piloid areas (**h**); histologically malignant component with nuclear hyperchromasia, hypercellularity and mitoses (*arrows*) (**i**)

*PTEN*-deleted and non-deleted tumors, or between pAKT/pS6 immunohistochemistry. However, there was an increase in pS6 staining in *PTEN*-deleted versus non-deleted tumors.

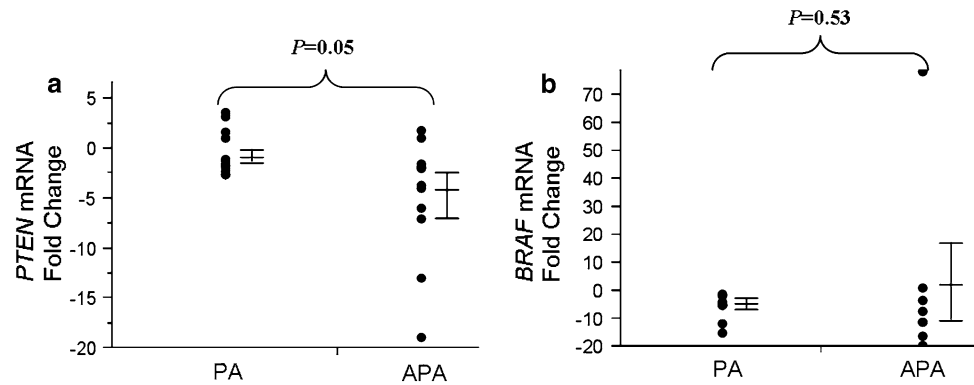
#### *PI3K/AKT pathway*

Using phospho-specific antibodies reflecting activation of the MAPK/ERK and PI3K/AKT pathways, immunohistochemical studies were undertaken (Fig. 4). A stepwise

increase in pAKT staining in clinically aggressive/recurrent PA and histologically anaplastic PA was noted when compared with conventional PA (respectively,  $p = 0.02$  and  $p = 0.006$ ). Although the staining for total AKT was weak, this was uniform in all tumor groups ( $p > 0.05$ ). This finding could be related to differences in antibody sensitivity between AKT and pAKT, but support that the increases in the latter are due to phosphorylation rather than a simple increase in total levels. pS6 staining intensity was also increased in histologically anaplastic PA when



**Fig. 3** Decreased *PTEN* gene expression in histologically anaplastic PA (APA). Decreased levels of *PTEN* mRNA were identified by qRT-PCR in a subset of APA tumors ( $n = 11$ ) when compared with conventional PA ( $n = 17$ ) (a). In contrast, there was no difference in *BRAF* mRNA levels between the two groups (b) (Wilcoxon Rank-Sum; error bars SEM)



compared with conventional PA ( $p = 0.005$ ), but there was only a non-significant trend for increased staining when compared with aggressive/recurrent PA ( $p = 0.09$ ). In contrast, pERK staining intensity was similarly increased in all three PA groups, a reflection of consistent activation of MAPK/ERK signaling in astrocytomas of all types and grades. When comparing pERK/pS6/pAKT staining between conventional and anaplastic components of the same tumor (in the same resection or prior precursor) or between the precursor and recurrence in recurrent/clinically aggressive PA (available in 13, 10, and 12 cases, respectively), we found that in most instances, increased staining was present in the precursors. These findings suggest that activation of these pathways is an early feature of clinical aggressiveness/anaplasia in these tumors.

#### Cellular proliferation and p53

Quantification of MIB1-labeling indices showed increased cell proliferation in histologically anaplastic PA when compared with conventional as well as aggressive/recurrent PA ( $p < 0.001$ ). No difference was noted between conventional and aggressive/recurrent PA ( $p = 0.31$ ) (Fig. 5). In addition, there was an association between increased MIB1-labeling indices and pAKT immunostaining ( $p = 0.008$ ). There was a trend for increased p53 nuclear staining in histologically anaplastic PA, but no stepwise increase was seen between the three groups ( $p > 0.05$ ).

#### Survival analyses

Overall survival decreased from conventional through clinically aggressive/recurrent PA to histologically anaplastic PA, with anaplasia remaining the strongest adverse prognostic factor ( $p < 0.001$ ) (Fig. 6a). pAKT staining was also associated with decreased survival in all groups combined after adjusting by extent of resection, age and location, but not when adjusting for clinical and histologic aggressiveness (Fig. 6b). Other features showing an

inverse association with overall survival on univariate analyses included increasing age, MIB1-labeling index, and extent of resection (gross total vs. subtotal/biopsy only) ( $p < 0.05$ ). Only age and extent of resection remained statistically significant after adjusting by histologic anaplasia ( $p < 0.05$ ).

#### Discussion

Activation of the PI3K/AKT and MAPK/ERK pathways by various molecular mechanisms is ubiquitous in a variety of malignancies, including high grade astrocytomas [18]. Our study evaluated the association of alterations of these pathways with various PA subsets. In recent years, several studies have highlighted the importance of MAPK/ERK activation in the pathobiology of PA. Activation occurs most frequently by alterations in the *BRAF* gene, particularly a tandem duplication of its kinase domain resulting in a *BRAF:KIAA1549* gene fusion [15]. More recently, a similar duplication–fusion event was reported in a minority of PA involving *RAF1* and *SRGAP3* genes [16]. Other less specific alterations reported in PA include the *BRAF*<sup>V600E</sup> point mutation, which leads to constitutive activation of BRAF. *BRAF*<sup>V600E</sup> may more often be found in pediatric diffuse gliomas [27] and gangliogliomas [6]. The *BRAF*<sup>V600E</sup> mutation also occurs in melanoma and papillary thyroid carcinoma.

In PA developing in the context of NF1 disease, homozygous inactivation of the *NF1* gene is an alternative mechanism for MAPK/ERK activation and seems to be a mutually exclusive alternative to *BRAF* mutation [34]. Although NF1-associated PA seems to be associated with a better outcome when compared with its sporadic counterpart, associations of *BRAF* aberrations with prognosis have been less consistent [8, 13, 15, 22]. Of note, 28% of the histologically anaplastic PA in our series were NF1-associated and not related to the optic pathways. Although NF1-associated PA tend to have a better outcome when compared with their sporadic counterparts, this is highlighted

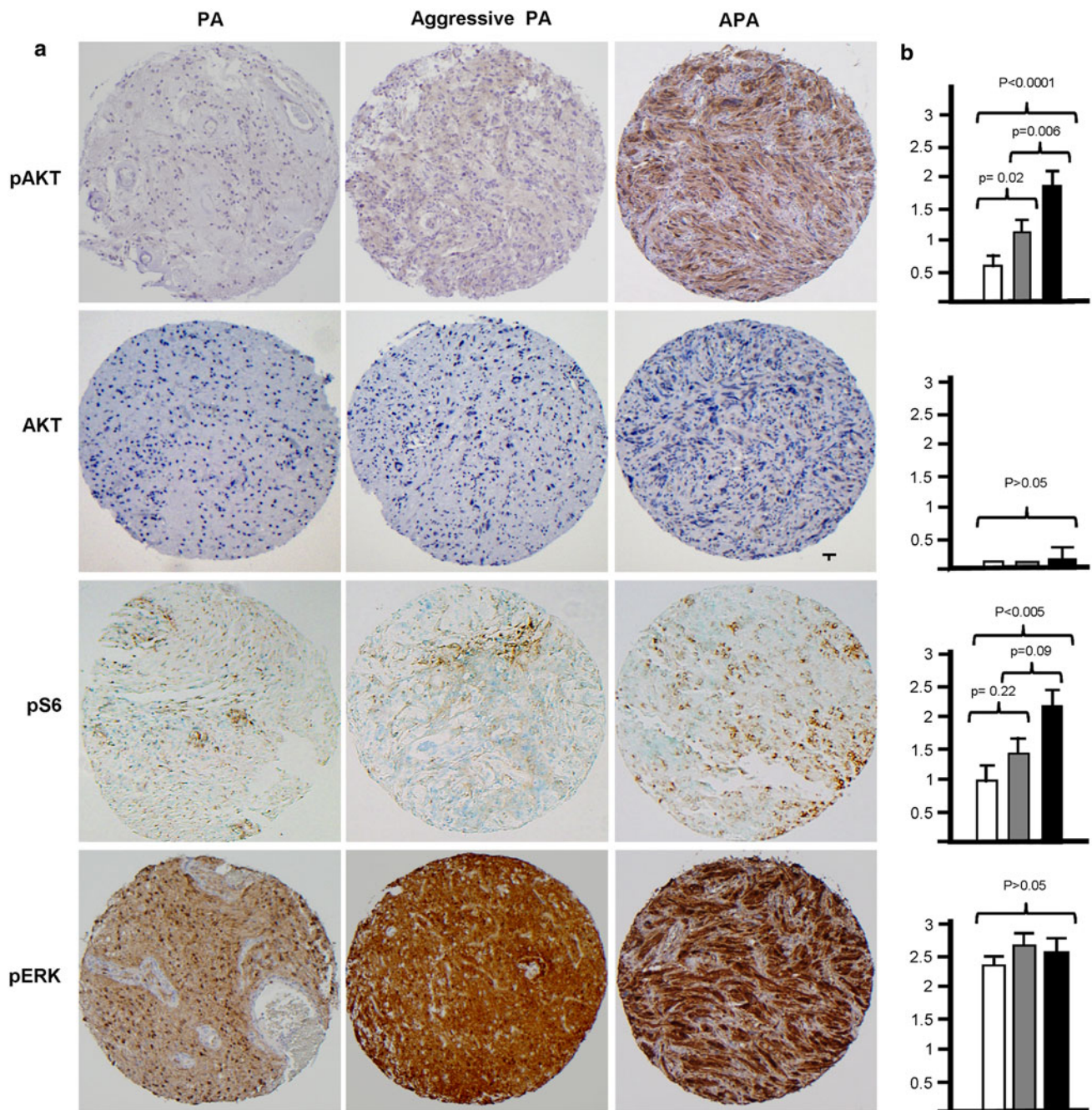


**Fig. 4** AKT pathway signaling is increased in histologically anaplastic PA (APA) when compared with conventional and clinically aggressive PA. Tissue microarray sections stained with immunohistochemistry using total protein and phospho-specific antibodies (a).

Semiquantification results corresponding to the immunohistochemistry tests are illustrated on the right (b) (white bars conventional PA; gray bars clinically aggressive PA; black bars APA(B) (Wilcoxon rank sum, error bars SEM)

more in optic pathway tumors, which may even spontaneously regress, and are usually not resected in most instances at the current time [20, 24]. The optic pathway, at the biologic level, represents a unique niche in NF1 [33], with a low potential for clinical and histological progression, explaining in part the absence of these tumors in our series.

However, infiltrating and high grade astrocytomas may occur throughout the neuraxis in NF1, especially in older patients, and be associated with similar molecular abnormalities and adverse outcome as their sporadic counterparts [11, 24]. Another possible explanation for the increased prevalence of NF1 cases in our series is that they are

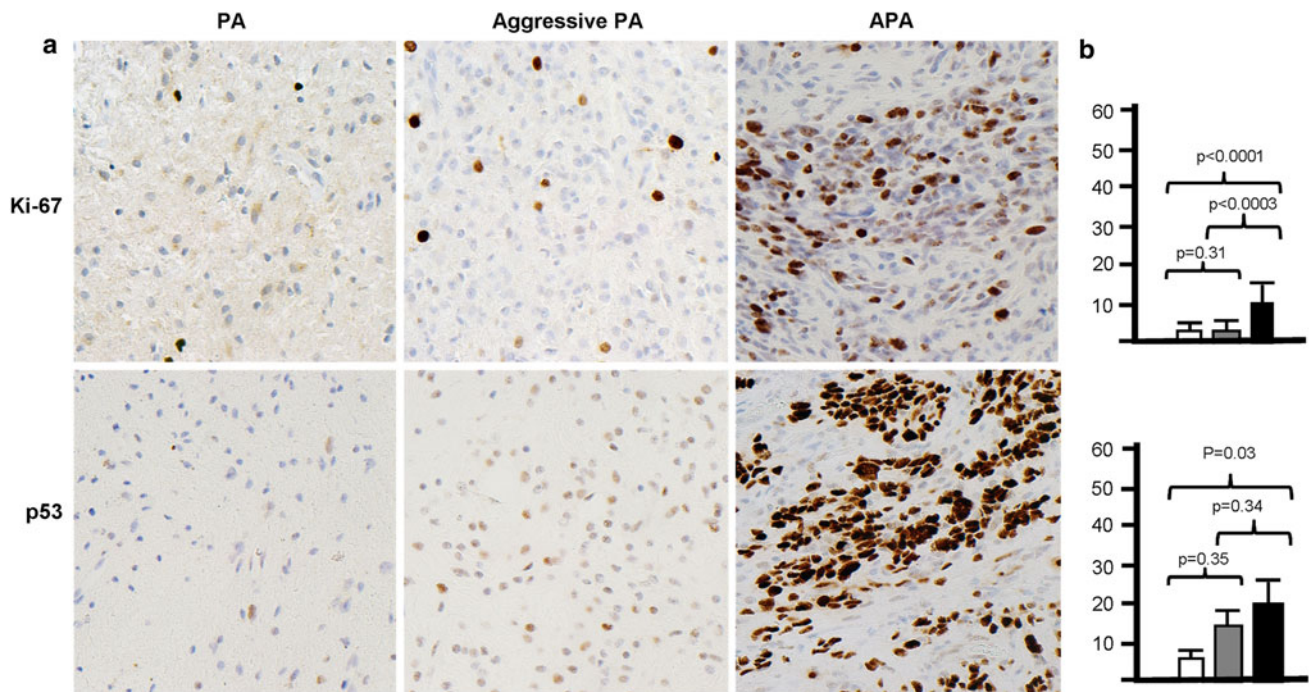
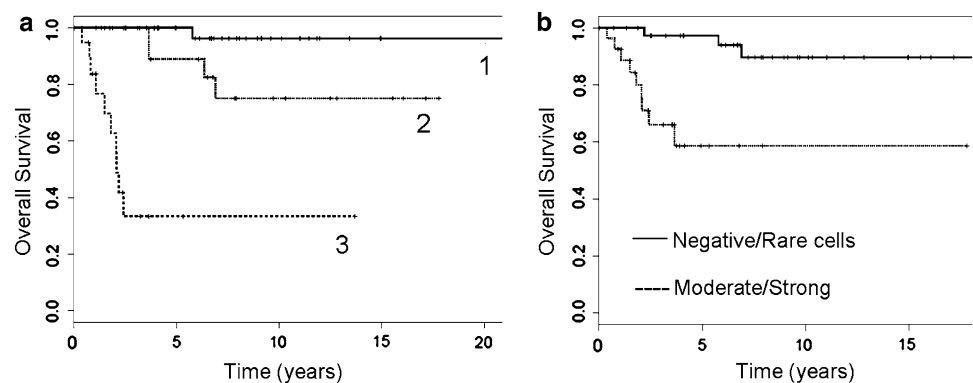


**Fig. 5** Increased cellular proliferation in histologically anaplastic PA (APA) when compared with aggressive and conventional PA. MIB1 and p53 nuclear immunostains in conventional PA, aggressive PA, and APA. Increased MIB1-labeling indices, in particular, are a feature of APA (a). Increased p53 staining was present in some histologically anaplastic PA, but the differences between the groups were not as

evident as proliferation and pAKT staining. Re-review of the histology of this specific case demonstrating strong p53 staining (b) showed classic pilocytic histology in part of the tumor (Case 6, Fig. 2) (white bars conventional PA, gray bars clinically aggressive PA, black bars APA (Wilcoxon rank sum, error bars SEM)

**Fig. 6** Histologic anaplasia and AKT activation are associated with decreased overall survival in PA. Kaplan–Meier curves illustrate decrease survival in APA (3) when compared with clinically aggressive (2) and conventional PA (1) ( $p < 0.005$ , Log rank test) (a). Higher levels of pAKT as assessed by immunohistochemistry are also associated with decreased survival in PA ( $p < 0.001$ ) (b)



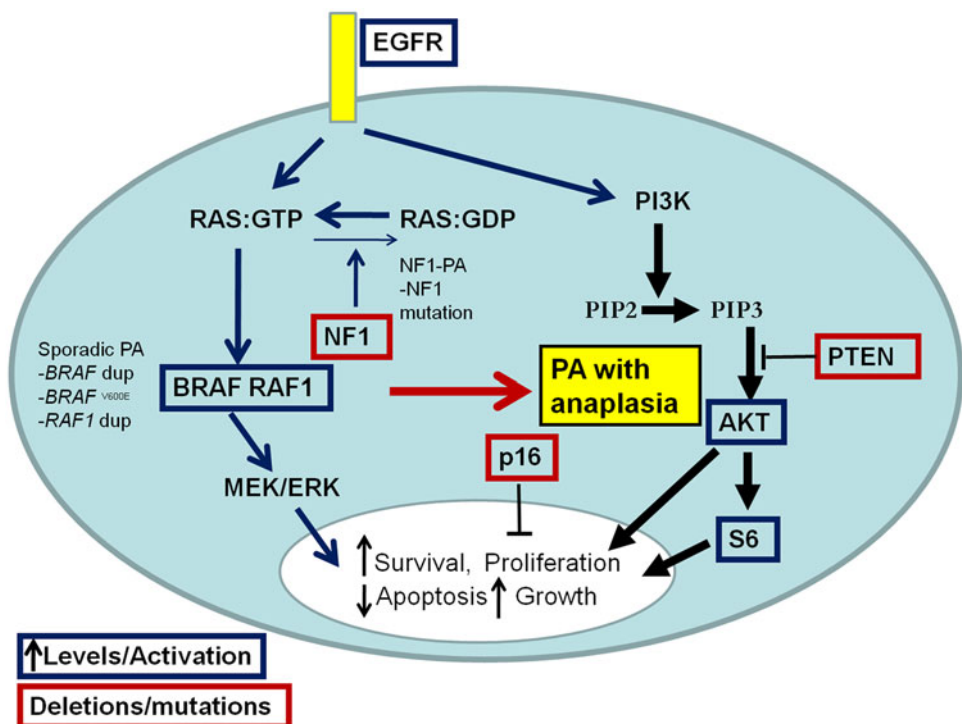
predominantly consultation derived, and NF1-associated tumors other than PA, especially with unusual morphologies, are more likely to be shared in consultation.

It is of interest that *BRAF* duplications were identified in 63% of the cerebellar anaplastic PA, but in none of seven non-cerebellar examples. This may suggest that non-cerebellar anaplastic PA may activate the ERK pathway by alternative mechanisms, in spite of similar histology, which may involve, among other alterations, point mutations (e.g. *RAS*) or *RAF1* rearrangements as previously described in a minority of PA [16, 30]. In addition, only 40% of the sporadic non-anaplastic PA in our series showed *BRAF*

duplication, although this alteration was present in almost half (47%) of posterior fossa examples. Variation in *BRAF* aberration frequency according to anatomic site has been reported, with prior studies showing a decreased frequency of *BRAF* rearrangements in non-cerebellar examples [34], down to 38% in one study [12]. In addition, *BRAF* rearrangements may also be associated with lower patient age [12], which can in part explain the lower prevalence in our relatively older patient population.

Although clinical observations and prior studies both noted aggressive clinical behavior in a subset of PA showing otherwise conventional histology [5], molecular

**Fig. 7** Model of molecular mechanisms underlying PA and histologically anaplastic PA. RAS/BRAF/MEK pathway activation by various mechanisms is a key feature of sporadic PA and NF1 PA. Histologically anaplastic PA develop in addition hyperactivation of the PI3K/PTEN/AKT pathway and inactivation of cell cycle inhibitors such as p16 leading to increased proliferation



abnormalities associated with the worse outcome remained elusive, comprehensive gene expression studies demonstrating no global changes reliably distinguishing conventional from clinically aggressive PA [28]. However, alterations in specific genes and proteins associated with a clinically aggressive phenotype were noted including increased levels of matrilin-2 [29] and decreased levels of ALDH1L1 [23].

Recent studies have also explored the relationship of various molecular alterations and outcome in PA. Tibbetts et al. [32] did not find an association with recurrence free survival in PA with respect to ERK or mTOR activation. However, their study did not include histologically anaplastic PA, which had the highest degree of pS6 staining in our study, and AKT activation (pAKT) was not tested. At difference with our study, Horbinski et al. [12] found homozygous *p16* deletions by FISH in 6% of PA and LOH at the *PTEN* locus in 50% by PCR-based microsatellite LOH analysis, findings not associated with adverse outcome. Their study also did not include histologically anaplastic PA, and the prevalence of homozygous *p16* deletions was higher in this cohort (20%) in our study. With respect to *PTEN*, we did not find heterozygous deletions by FISH in non-anaplastic PA, but in 32% of histologically anaplastic PA. These findings suggest that even though *PTEN* LOH may be found in conventional PA, large deletions identified by FISH may be more closely associated with anaplastic histology.

Amplifications of receptor tyrosine kinases are important genetic events in the development of high-grade astrocytomas. *EGFR* amplification is most frequently seen in primary glioblastomas of adults, while *PDGFRA* amplification has been identified in a subset of pediatric high-grade astrocytomas [21]. In our study, we did not encounter these aberrations.

In the current study, we demonstrate that, in addition to MAPK/ERK pathway activation, increased PI3K/AKT activity also seems to be a feature of clinically aggressive PA and particularly histologically anaplastic PA. A possible model summarizing these findings is illustrated in Fig. 7. Notably, however, NF1-associated tumors, including PA, are associated with increased mTOR pathway signaling [4, 14]. In addition to aberrations of MAPK/ERK, histologically anaplastic PA develop alterations characteristic of high grade astrocytomas, including heterozygous *PTEN/10q* and homozygous *p16* deletions. Frequent alterations in the PTEN/PI3K/AKT pathway were also noted in a prior study of malignant transformation in pediatric low grade gliomas [3], although only one example progressed from a PA.

Although the status of the remaining *PTEN* allele was not tested in our study, decreased expression of the gene at the mRNA level in histologically anaplastic PA suggests that this aberration may have biological significance. Furthermore, it seems to occur early in their evolution, being present in two (of 2) cases in which the PA precursors were

tested. Our findings also reinforce recent findings highlighting the importance of *PTEN* loss in malignant progression of other NF1-associated tumors, particularly neurofibromas progressing to malignant peripheral nerve sheath tumors [10]. Now, in the current study, we were unable to demonstrate a definite relationship between *PTEN* deletion, *PTEN* gene underexpression and pAKT/pS6 immunohistochemistry, even though each of these variables was more prevalent in histologically anaplastic PA. This suggests that alternative mechanisms to *PTEN* loss may also activate AKT signaling in histologically anaplastic PA, in a similar way to other astrocytomas that have mutations in other PI3K pathway components [18]. Future studies should be more illustrative in this regard.

PI3K/AKT activation underlies increased cellular proliferation characteristic of anaplasia and an adverse histologic phenotype in PA. Indeed, an inverse relation between MIB1-labeling index and progression-free survival was noted in one prior study of PA [2]. Interestingly, a worsening of prognosis with increased MIB1 labeling was not confirmed by other studies [5, 7, 9]. We did not identify a significant difference in MIB1-labeling indices between clinically aggressive/recurrent PA and conventional PA, but did find a significant increase in histologically anaplastic PA. These findings support the notion that increased cellular proliferation is an important, defining trait of histologic anaplasia in PA and a factor underlying the worse prognosis associated with these tumors.

In summary, this study assessed the prevalence of key molecular genetic abnormalities in clinically and histologically aggressive PA, and highlighted important differences in PA subsets with respect to PI3K/AKT activation status. Further, more comprehensive studies should confirm these findings and identify additional molecular aberrations in aggressive PA subsets, perhaps identifying therapeutic targets beneficial to astrocytoma patients in general.

**Acknowledgments** This work was funded in part by grant P50 CA108961 from the Mayo SPORE in Brain Cancer (CG, FJR, JNS) and Mayo Clinic CTSA (FJR) through grant number UL1 RR024150 from the National Center for Research Resources (NCRR), a component of the National Institutes of Health (NIH). The authors also thank the microarray, tissue, cell molecular analysis and cytogenetic shared resources of the Mayo Clinic for excellent technical assistance.

## References

- Bar EE, Lin A, Tihan T, Burger PC, Eberhart CG (2008) Frequent gains at chromosome 7q34 involving BRAF in pilocytic astrocytoma. *J Neuropathol Exp Neurol* 67:878–887
- Bowers DC, Gargan L, Kapur P et al (2003) Study of the MIB-1 labeling index as a predictor of tumor progression in pilocytic astrocytomas in children and adolescents. *J Clin Oncol* 21:2968–2973
- Broniscer A, Baker SJ, West AN et al (2007) Clinical and molecular characteristics of malignant transformation of low-grade glioma in children. *J Clin Oncol* 25:682–689
- Dasgupta B, Yi Y, Chen DY, Weber JD, Gutmann DH (2005) Proteomic analysis reveals hyperactivation of the mammalian target of rapamycin pathway in neurofibromatosis 1-associated human and mouse brain tumors. *Cancer Res* 65:2755–2760
- Dirven CM, Mooij JJ, Molenaar WM (1997) Cerebellar pilocytic astrocytoma: a treatment protocol based upon analysis of 73 cases and a review of the literature. *Childs Nerv Syst* 13:17–23
- Dougherty MJ, Santi M, Brose MS et al (2010) Activating mutations in BRAF characterize a spectrum of pediatric low-grade gliomas. *Neuro Oncol* 12:621–630
- Fisher BJ, Naumova E, Leighton CC et al (2002) Ki-67: a prognostic factor for low-grade glioma? *Int J Radiat Oncol Biol Phys* 52:996–1001
- Forshew T, Tatevossian RG, Lawson AR et al (2009) Activation of the ERK/MAPK pathway: a signature genetic defect in posterior fossa pilocytic astrocytomas. *J Pathol* 218:172–181
- Giannini C, Scheithauer BW, Burger PC et al (1999) Cellular proliferation in pilocytic and diffuse astrocytomas. *J Neuropathol Exp Neurol* 58:46–53
- Gregorian C, Nakashima J, Dry SM et al (2009) PTEN dosage is essential for neurofibroma development and malignant transformation. *Proc Natl Acad Sci USA* 106:19479–19484
- Gutmann DH, Rasmussen SA, Wolkenstein P et al (2002) Gliomas presenting after age 10 in individuals with neurofibromatosis type 1 (NF1). *Neurology* 59:759–761
- Horbinski C, Hamilton RL, Nikiforov Y, Pollack IF (2010) Association of molecular alterations, including BRAF, with biology and outcome in pilocytic astrocytomas. *Acta Neuropathol* 119:641–649
- Jacob K, Albrecht S, Sollier C et al (2009) Duplication of 7q34 is specific to juvenile pilocytic astrocytomas and a hallmark of cerebellar and optic pathway tumours. *Br J Cancer* 101:722–733
- Johannessen CM, Reczek EE, James MF, Brems H, Legius E, Cichowski K (2005) The NF1 tumor suppressor critically regulates TSC2 and mTOR. *Proc Natl Acad Sci USA* 102:8573–8578
- Jones DT, Kocialkowski S, Liu L et al (2008) Tandem duplication producing a novel oncogenic BRAF fusion gene defines the majority of pilocytic astrocytomas. *Cancer Res* 68:8673–8677
- Jones DT, Kocialkowski S, Liu L, Pearson DM, Ichimura K, Collins VP (2009) Oncogenic RAF1 rearrangement and a novel BRAF mutation as alternatives to KIAA1549:BRAF fusion in activating the MAPK pathway in pilocytic astrocytoma. *Oncogene* 28:2119–2123
- Nakamura N, Carney JA, Jin L et al (2005) RASSF1A and NRE1A methylation and BRAFV600E mutations in thyroid tumors. *Lab Invest* 85:1065–1075
- Network TCGA (2008) Comprehensive genomic characterization defines human glioblastoma genes and core pathways. *Nature* 455:1061–1068
- Ohgaki H, Kleihues P (2005) Population-based studies on incidence, survival rates, and genetic alterations in astrocytic and oligodendroglial gliomas. *J Neuropathol Exp Neurol* 64:479–489
- Parsa CF, Hoyt CS, Lesser RL et al (2001) Spontaneous regression of optic gliomas: thirteen cases documented by serial neuroimaging. *Arch Ophthalmol* 119:516–529
- Paugh BS, Qu C, Jones C et al (2010) Integrated molecular genetic profiling of pediatric high-grade gliomas reveals key differences with the adult disease. *J Clin Oncol* 28:3061–3068

22. Pfister S, Janzarik WG, Remke M et al (2008) BRAF gene duplication constitutes a mechanism of MAPK pathway activation in low-grade astrocytomas. *J Clin Invest* 118:1739–1749
23. Rodriguez FJ, Giannini C, Asmann YW et al (2008) Gene expression profiling of NF-1-associated and sporadic pilocytic astrocytoma identifies aldehyde dehydrogenase 1 family member L1 (ALDH1L1) as an underexpressed candidate biomarker in aggressive subtypes. *J Neuropathol Exp Neurol* 67:1194–1204
24. Rodriguez FJ, Perry A, Gutmann DH et al (2008) Gliomas in neurofibromatosis type 1: a clinicopathologic study of 100 patients. *J Neuropathol Exp Neurol* 67:240–249
25. Rodriguez FJ, Scheithauer BW, Burger PC, Jenkins S, Giannini C (2010) Anaplasia in pilocytic astrocytoma predicts aggressive behavior. *Am J Surg Pathol* 34:147–160
26. Rodriguez FJ, Scheithauer BW, Giannini C, Bryant SC, Jenkins RB (2008) Epithelial and pseudoepithelial differentiation in glioblastoma and gliosarcoma: a comparative morphologic and molecular genetic study. *Cancer* 113:2779–2789
27. Schiffman JD, Hodgson JG, VandenBerg SR et al (2010) Oncogenic BRAF mutation with CDKN2A inactivation is characteristic of a subset of pediatric malignant astrocytomas. *Cancer Res* 70:512–519
28. Sharma MK, Mansur DB, Reifenberger G et al (2007) Distinct genetic signatures among pilocytic astrocytomas relate to their brain region origin. *Cancer Res* 67:890–900
29. Sharma MK, Watson MA, Lyman M et al (2006) Matrilin-2 expression distinguishes clinically relevant subsets of pilocytic astrocytoma. *Neurology* 66:127–130
30. Sharma MK, Zehnbauer BA, Watson MA, Gutmann DH (2005) RAS pathway activation and an oncogenic RAS mutation in sporadic pilocytic astrocytoma. *Neurology* 65:1335–1336
31. Sievert AJ, Jackson EM, Gai X et al (2009) Duplication of 7q34 in pediatric low-grade astrocytomas detected by high-density single-nucleotide polymorphism-based genotype arrays results in a novel BRAF fusion gene. *Brain Pathol* 19:449–458
32. Tibbetts KM, Emnett RJ, Gao F, Perry A, Gutmann DH, Leonard JR (2009) Histopathologic predictors of pilocytic astrocytoma event-free survival. *Acta Neuropathol* 117:657–665
33. Warrington NM, Woerner BM, Daginakatte GC et al (2007) Spatiotemporal differences in CXCL12 expression and cyclic AMP underlie the unique pattern of optic glioma growth in neurofibromatosis type 1. *Cancer Res* 67:8588–8595
34. Yu J, Deshmukh H, Gutmann RJ et al (2009) Alterations of BRAF and HIPK2 loci predominate in sporadic pilocytic astrocytoma. *Neurology* 73:1526–1531